Excitation of Spin Waves in an In-Plane-Magnetized Ferromagnetic Nanowire Using Voltage-Controlled Magnetic Anisotropy

Roman Verba, Mario Carpentieri, Giovanni Finocchio, Vasil Tiberkevich, and Andrei Slavin

Phys. Rev. Applied **7**, 064023 — Published 16 June 2017

DOI: 10.1103/PhysRevApplied.7.064023

Excitation of spin waves in an in-plane magnetized ferromagnetic nanowire using voltage-controlled magnetic anisotropy

Roman Verba,[1,*] Mario Carpentieri,[2] Giovanni Finocchio,[3] Vasil Tiberkevich,[4] and Andrei Slavin[4]

[1]*Institute of Magnetism, Kyiv 03680, Ukraine*

[2]*Department of Electrical and Information Engineering, Politecnico di Bari, I-70125 Bari, Italy*

[3]*Department of Electronic Engineering, Industrial Chemistry and Engineering, University of Messina, I-98166 Messina, Italy*

[4]*Department of Physics, Oakland University, Rochester, MI 48309, USA*

(Dated: May 18, 2017)

It is demonstrated by analytical calculations and micromagnetic simulations that a microwave pumping by means of a voltage-controlled magnetic anisotropy (VCMA) could excite propagating spin waves in a ferromagnetic nanowire with in-plane static magnetization, and only the parametric excitation is possible. The efficiency of the parametric excitation is proportional to the out-of-plane component of the dynamic magnetization, and is non-vanishing in all the range of spin wave wave vectors. This property ensures the excitation of spin waves in a wide frequency range (up to tens of gigahertz) using practically achievable amplitudes of the VCMA pumping. For a Fe/MgO nanowire the threshold of parametric excitation of spin waves lies in the range 0.5-1 V/nm and only weakly depends on the nanowire width.

I. INTRODUCTION

The effect of voltage-controlled magnetic anisotropy (VCMA) manifests itself as a variation of the perpendicular magnetic anisotropy at the interface between a ferromagnetic metal and dielectric under the action of an electric field applied to the interface [1–3]. Similar to other magnetoelectric effects, e.g. in piezoelectric-piezomagnetic heterostructures, the effect of VCMA could provide an effective control of the magnetization in a ferromagnetic material with very low power consumption [4–6], much lower than using well-developed methods of magnetization control by magnetic field or electric current. The useful and convenient features of the VCMA effect, such as the technological simplicity of its application at nanoscale, high performance, and linearity as a function of the applied electric field [7–10] make VCMA one of the most attractive magnetoelectric effect for the application in spintronics and spin-wave (SW)-based signal processing, which attract significant research interest currently [11, 12]. In particular, the VCMA effect has been already proposed and tested for the application in magnetic recording [13, 14], motion control of domain wall [15, 16], skyrmions [17–19] and spin waves [20], and for the excitation of the ferromagnetic resonance [9, 10, 21].

In our previous works [22, 23], we have shown both by analytical calculations and by micromagnetic simulations that microwave pumping by means of the VCMA could excite propagating SWs in an ultrathin ferromagnetic nanowire with an out-of-plane (OOP) static magnetization. In that case VCMA pumping leads to the variation of the OOP component of the effective magnetic field, which is parallel to the static magnetization (so called "parallel pumping geometry"[24]). Thus, in the case of the OOP magnetization the SWs cannot be excited in a common linear regime, when the frequencies of driving signal and SWs are the same. Instead, the parametric excitation – a well-known method of SW excitation, when the frequency of pumping is twice larger than the frequency of the excited SW [24–26] – is possible.

For practical applications it is very desirable to use devices without permanent magnetic field bias. It is known, that the static state of unbiased ultrathin ferromagnetic films and nanowires depends often on their thickness – below a certain critical thickness the static magnetization is OOP, above this thickness – in-plane (IP) [27, 28]. The critical value depends on the perpendicular surface magnetic anisotropy and the saturation magnetization, and, typically, is of the order of 1 nm. Here we show that in the case of the IP magnetization, as in the case of the OOP magnetization, only the parametric excitation of SWs is possible. It is also shown that the parametric excitation in thicker IP-magnetized magnetic nanowires could be more efficient than in thinner OOP-magnetized nanowires, despite the fact that VCMA is a purely interface effect, and, therefore, its efficiency decreases with the increase of the nanowire thickness.

The relatively high efficiency of SW parametric excitation is not the only advantage of the IP-magnetized thicker nanowires. Thicker nanowires are, usually, easier to fabricate, and they have better uniformity. Therefore, thicker IP-magnetized nanowires have a lower inhomogeneous broadening of the SW linewidth [29]. Due to the vanishing static demagnetization fields, in the case of the IP magnetization it is possible to achieve higher SW frequency at zero bias field. Also, the IP-magnetization geometry allows one to combine the VCMA-based SW excitation with the advantages of the interfacial Dzyaloshinsii-Moriya interaction (IDMI), which takes place in ferromagnetic films grown on a heavy metal substrate [30, 31]. The IDMI is known to result in the nonreciprocal SW propagation [30, 32, 33], and the

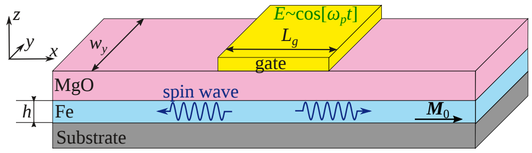

FIG. 1. A layout of the Fe-MgO nanowire with VCMA excitation gate.

largest nonreciprocity is achieved for the case of the IP-magnetization, while for the OOP static magnetization nonreciprocity is absent [33, 34]. Obviously, the nonreciprocity of the SW propagation could provide additional functionality of the SW signal processing devices [35].

II. THEORY

The considered layered structure is shown in Fig. 1. It consists of a thin layer of a ferromagnetic metal (e.g. Fe) covered by a dielectric layer (e.g. MgO) formed as a nanowire of the width w_y. The metal excitation gate of the length L_g is placed on top of the nanowire. The static magnetization of ferromagnetic layer lies in-plane along the nanowire length (x-axis). Below we use the material parameters of a Fe-MgO structure, which is often used in the VCMA experiments: saturation magnetization of $\mu_0 M_s = 2.1\,\mathrm{T}$, exchange length $\lambda_{ex} = 3.4\,\mathrm{nm}$, perpendicular surface anisotropy energy $K_s = 1.36\,\mathrm{mJ/m^2}$, Gilbert damping $\alpha_G = 0.004$, nonuniform line broadening $\Delta\omega_{nu} = 2\pi \times 230\,\mathrm{MHz}$, magnetoelectric coefficient $\beta_s = 100\,\mathrm{fJ/(V*m)}$ [28, 29, 36]. The thickness of the Fe layer was chosen to be $h = 1\,\mathrm{nm}$. Used parameters are the same as in Ref. 22, except for the thickness (critical thickness, corresponding to the OOP to IP state transition for Fe/MgO film is $h_{cr} = 2K_s/(\mu_0 M_s^2) = 0.78\,\mathrm{nm}$, and slightly increases for nanowires), that allows us to compare excitation efficiency in the OOP and the IP geometry.

Magnetization dynamics in a nanowire is described by Landau-Lifshitz equation for the magnetization vector $\boldsymbol{M}(\boldsymbol{r},t)$:

$$\frac{\partial \boldsymbol{M}}{\partial t} = -\gamma \boldsymbol{M} \times \boldsymbol{B}_{eff} - \frac{\gamma \alpha_G}{M_s} \boldsymbol{M} \times (\boldsymbol{M} \times \boldsymbol{B}_{eff}) \;, \quad (1)$$

where γ is the gyromagnetic ratio, α_G is Gilbert damping constant (strictly speaking, effective, see below), M_s is the saturation magnetization and $\boldsymbol{B}_{eff}$ is the effective field consisting of external field (absent in our case), exchange, anisotropy and magnetodipolar contributions. The variable microwave electric field $E(t) \sim \cos[\omega_p t]$ at the frequency ω_p, applied to the excitation gate, creates the variation of the perpendicular surface anisotropy $\Delta K_s = \beta E$. Corresponding variation of the effective field $\Delta \boldsymbol{B}_{eff}$ can be found as a variational derivative of the anisotropy energy density $W_{an} = -\Delta K_s M_z^2/(h M_s^2)$:

$$\Delta \boldsymbol{B}_{eff}(t,\boldsymbol{r}) = -\frac{\delta}{\delta \boldsymbol{M}} \left(-\frac{\beta E M_z^2}{h M_s^2} \right) = \frac{2\beta E(t,\boldsymbol{r}) M_z(t,\boldsymbol{r})}{h M_s^2} \boldsymbol{e}_z \,. \quad (2)$$

As one can see, the electrically driven component of the effective field is not orthogonal to the dynamic magnetization, since both of them have nonzero z-component, and, consequently, the effective field can linearly affect dynamic magnetization and SWs. This is in contrast to the case of the OOP static magnetization, for which $\Delta \boldsymbol{B}_{eff}$ (described by the same Eq. (2)) is parallel to the static magnetization. However, note, that $M_z(t)$ is the *dynamic* magnetization component having zero static value and varying at the frequency ω_k of the excited SW, if the excitation of SW takes place. Thus, there are no terms in the expression for $\boldsymbol{B}_{eff}$ proportional solely to the external force $E(t)$ and varying at the frequency of the external electric field. Consequently, the linear excitation of SW in this geometry is impossible, nevertheless microwave VCMA-induced effective field is perpendicular to the static magnetization. It could be shown that the linear excitation of SWs becomes possible if the nanowire is magnetized at finite angle to the surface $\theta_M \neq 0, \pi/2$ [10]. At the same time, if the variable electric field has the frequency component $\omega_p \approx 2\omega_k$, the effective magnetic field contains the *resonant* term at the SW frequency ω_k, and the *parametric* excitation of SWs may become possible.

To investigate SW dynamics we use a standard expansion of magnetization as the sum of static one and series of SW modes: $\boldsymbol{M}(\boldsymbol{r},t) = M_s \left[\boldsymbol{e}_x + \sum_{n,k} \left(c_{n,k} \boldsymbol{m}_{n,k} e^{i(kx - \omega_{n,k} t)} + \text{c.c.} \right) \right]$. SW modes are characterized by the wave vector $\boldsymbol{k} = k\boldsymbol{e}_x$ and quantization number $n = 0, 1, 2, ...$, which defines SW mode profile $\boldsymbol{m}_{n,k} = \boldsymbol{m}_{n,k}(y)$ in the y-direction (across the nanowire width). Substituting this representation in Eq. (1) one can obtain the following equation describing dynamics of SW mode amplitude c_k [37]:

$$\frac{dc_k}{dt} + i\omega_k c_k + \Gamma_k c_k = \sum_{k'=-\infty}^{\infty} \frac{L_g}{l_x} V_{kk'} \tilde{b}_{k+k'} e^{-i\omega_p t} c_{k'}^* \,. \quad (3)$$

Since pumping is uniform across the nanowire width, it doesn't lead to a coupling between modes with different width profiles (different n), and dynamics of SWs with certain definite n is described by the same Eq. (3). For this reason we omit index n in Eq. (3) and below. Value $\tilde{b}_k = L_g^{-1} \int b(x) e^{-ikx} dx$ in Eq. (3) is the Fourier image of a spatial profile of effective microwave pumping field $b(x) = 2\beta E(x)/(h M_s)$, l_x is the full length of the nanowire, Γ_k is the SW damping rate which includes the Gilbert damping and the nonuniform SW line broadening. Eq. (3) is absolutely the same as in the case of a parallel pumping [22, 37], but the efficiency of the parametric interaction for the resonant case ($k' = -k$) is now equal to

$$|V_{k(-k)}| = |V_{kk}| = \gamma \frac{\langle |m_{k,z}|^2 \rangle}{2A_k}. \quad (4)$$

Here $A_k = i\langle \boldsymbol{m}_k^* \cdot \boldsymbol{e}_x \times \boldsymbol{m}_k \rangle$ is the norm of the SW mode [38], symbols $\langle ... \rangle$ mean averaging over the nanowire width. As one can see, the efficiency of the parametric excitation of SWs V_{kk} is proportional to the *out-of-plane magnetization component* $m_{k,z}$, and not to the difference of dynamic magnetization components $\langle |m_{k,y}|^2 - |m_{k,z}|^2 \rangle$, as it is the case for the usual parallel pumping (see e.g. [37]). The appearance of such a dependence follows from Eq. (2). Indeed, $\boldsymbol{\Delta B}_{eff}$ is proportional to z-component of dynamic magnetization and has only z-component, acting, thus, on dynamical magnetization component m_z. In total, this results in the dependence $V_{kk} \sim |m_{k,z}|^2$. Eq. (4) is one of the key results of this work, it remains valid for any in-plane direction of static magnetization of nanowire. We'd like to note, that parametric coupling with efficiency like Eq. (4) cannot be realized by microwave magnetic field and is intrinsic for anisotropy pumping.

For the lowest SW mode, which is uniform along the nanowire width, Eq. (4) is simplified to

$$|V_{kk}| = \frac{\gamma}{4} \frac{|m_{k,z}|}{|m_{k,y}|} = \frac{\gamma}{4} \sqrt{\frac{\gamma B + \omega_M (\lambda_{ex}^2 k^2 + F_k^{(yy)})}{\gamma (B - B_{an}) + \omega_M (\lambda_{ex}^2 k^2 + F_k^{(zz)})}}, \quad (5)$$

where B is the static internal field in the nanowire, $\hat{\boldsymbol{F}}_k$ is the dynamic demagnetization tensor [22] and $B_{an} = 2K_s/(M_s h)$ is the anisotropy field. The wave number dependence of the parametric interaction efficiency V_{kk} for the lowest SW mode is shown in Fig. 2. The efficiency V_{kk} increases as the excited SW becomes shorter, and saturates at the value $\gamma/4$ in the high-k range due to the circular polarization of SWs ($|m_{k,y}| = |m_{k,z}|$, the limit $\lambda_{ex} k \gg 1$ in Eq. (5)) in this range of wave numbers. Thus, in the case of the in-plane magnetization, there are no principal restrictions on the wave number of the excited SW. This property is in a sharp contrast with the case of the OOP magnetization, where the excitation efficiency V_{kk} could have a zero value at a certain wave number and vanishes completely at high wave numbers k [22]. For small values of the SW wave number k the interaction efficiency is higher in narrower nanowires, as they have stronger in-plane demagnetization fields resulting in higher OOP dynamic magnetization (larger $F_k^{(yy)}$ component).

It is well-known, that the parametric excitation of SWs is a threshold excitation – the SWs are excited only if the pumping strength overcomes a certain threshold [24]. The minimum possible excitation threshold is equal to $b_{th} = \Gamma_k / V_{kk}$, and is realized in the case of relatively large gate size, $L_g \gg \Gamma_k / v$ (where v is the SW group velocity), and when the pumping frequency is twice larger

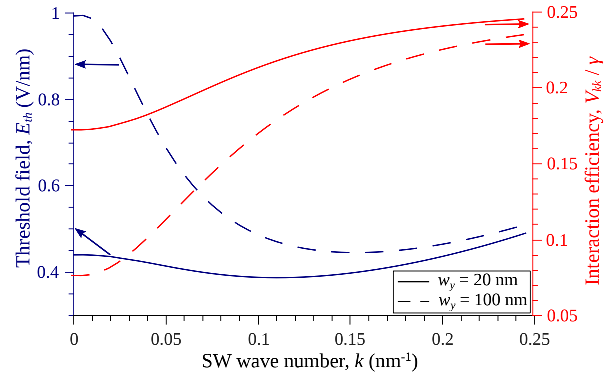

FIG. 2. Minimum parametric excitation threshold (left axis) and efficiency of the VCMA-induced parametric interaction of spin waves (right axis) as functions of the SW wave number for different widths of the ferromagnetic nanowire waveguide. Calculations were made for the lowest, uniform across the nanowire width, SW mode. Arrows show which curves belong to which axes.

than the frequency of the excited SW, $\omega_p = 2\omega_k$ (this condition, along with the SW dispersion law, determine the wave number of the excited SW). The corresponding threshold amplitude of the microwave electric field $E_{th} = b_{th} M_s h / 2\beta = \Gamma_k M_s h / (2\beta V_{kk})$ is shown in Fig. 2. It is clear, that in a relatively wide nanowire it is easier to excite relatively short SWs, while the excitation of SWs with $k \to 0$ requires a higher amplitude of the electric field pumping. In a relatively narrow nanowire this difference becomes less and less pronounced. Consequently, it is desirable to use the narrow nanowire waveguides, having the width of the order of 10-20 nm, only when working with small k, i.e. close to the ferromagnetic resonance (FMR) frequency. Away from the FMR (at a several GHz distance) the difference in the nanowire width is practically insignificant, as at $w_y > 30\,$nm the dependence of the parametric excitation threshold on the nanowire width saturates. This property also presents a contrast to the case of the OOP magnetization, where the SW excitation threshold increases linearly up to $w_y \sim 70 - 100\,$nm, so that the use of relatively narrow nanowires creates a significant advantage [22]. It should also be noted, that the minimum values of characteristic threshold in the case of the IP magnetization are similar to that in the OOP case (about 0.5 V/nm). However, the range of the excited SW frequencies is much larger. For example, for a 20 nm-wide waveguide the wave number range, shown in Fig. 2, in which the threshold varies insignificantly, corresponds to the SW frequency range $6\,\text{GHz} < \omega_k/2\pi < 50\,\text{GHz}$. In a nanowire with the same geometry (except for the thickness) and the OOP magnetization the excitation threshold is smaller than 1 V/nm only in the range 5-9 GHz [22]. Thus, excitation of relatively high-frequency SWs is more efficient in the IP magnetized case, that is a consequence of different coupling of the pumping to SWs.

Of course, for practical applications the excitation gate should have a finite length L_g, and the excited SWs should propagate from the gate to be processed and received by other gates. A finite gate length leads to the increase of the threshold, which is determined from following implicit equation [23]:

$$\frac{\sqrt{(Vb)^2-(\Gamma-\alpha Vb)^2}}{\Gamma-\alpha Vb}=-\tan\frac{\sqrt{(Vb)^2-(\Gamma-\alpha Vb)^2}L_g}{v}. \qquad (6)$$

Here $V = |V_{kk}|$ and $\alpha = |\tilde{b}_{2\boldsymbol{k}}/\tilde{b}_{\boldsymbol{0}}|$ is the so called "measure of the pumping non-adiabaticity", which describes interaction of co-propagating SWs with parametric pumping and is significant only when the pumping length L_g becomes comparable or less than SW wavelength [37]. In particular, for the case of a rectangular pumping profile $\alpha = |\mathrm{sinc}[kL_g]|$. The threshold increases from the minimum magnitude shown in Fig. 2, as the radiation losses $\Gamma_{rad} = v/L_g$ increase in comparison to the natural damping rate Γ_k, that is equivalent to increase of SW propagation length $l_p = v/\Gamma_k$ in comparison to the gate length L_g. In the limiting case of small gate length $L_g \ll l_p$, the threshold is equal to $b_{th}V_{kk} = \arccos(\alpha)\left(1+\alpha^2\right)^{-1/2} v/L_g$ [37]. For our parameters the maximum propagation path is achieved for SWs of the wavelength $2\pi/k \sim 20-30\,\mathrm{nm}$, and is about $l_p \approx 1\,\mu\mathrm{m}$.

III. MICROMAGNETIC SIMULATIONS

In order to verify the above presented theoretical predictions we performed micromagnetic simulations using the GPMagnet solver [39, 40]. The nanowire waveguide width was chosen to be $w_y = 20\,\mathrm{nm}$, the gate length was $L_g = 100\,\mathrm{nm}$, and the effective Gilbert constant was chosen to be $\alpha_G = 0.033$, which approximately takes into account both the real Gilbert damping and the nonuniform SW line broadening in the studied range of the SW frequencies. The thermal fluctuations corresponding to the temperature of $T = 1\,\mathrm{K}$ were also taken into account.

For these parameters the FMR frequency, which is the lowest frequency in the SW spectrum, is $\omega_0/2\pi = 6\,\mathrm{GHz}$. When the pumping frequency exceeds the double of the FMR frequency $\omega_p > 2\omega_0$, the propagating SWs can be excited at a certain threshold pumping amplitude, and above this threshold the amplitude of excited SW increases monotonically (Fig. 3). The wave number k of the parametrically excited SW is determined by the pumping frequency ($\omega_k = \omega_p/2$), and increases with the increase of the pumping frequency ω_p. Since the SW group velocity v also increases with the increase of the SW wave number k, the threshold of the SW excitation by a gate of a *finite length* increases with the increase of the ω_p.

Our simulations have also shown that the parametric

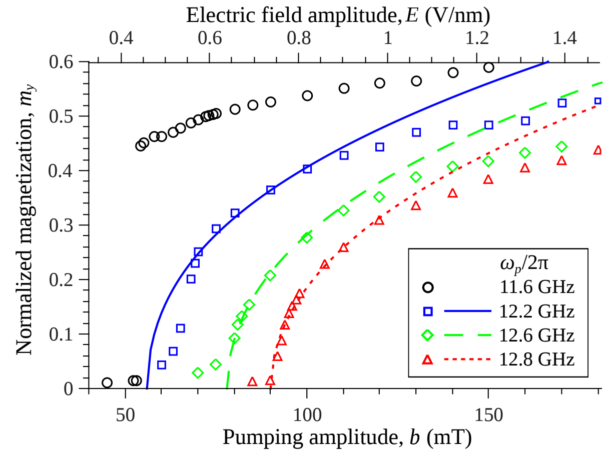

FIG. 3. Amplitudes of the excited SWs (normalized magnetization $m_y = M_y/M_s$ under the excitation gate center) as functions of the pumping strength: symbols – results of the micromagnetic simulations, lines – analytic theory.

excitation of SWs is possible even when the pumping frequency ω_p is slightly lower than the double FMR frequency (curve for 11.6 GHz in Fig. 3). However, in this case the SW excitation is of a "subcritical" type – the amplitude of the excited SW has a large finite value at the threshold. The excitation in this frequency range becomes possible due to nonlinear shift of SW frequency, which in our case is negative, that is common for thin films and nanowires with IP static magnetization [24, 41]. In this geometry the increase of the SW amplitude leads to the decrease of the SW frequency $\omega_k(|c_k|^2)$, so that the parametric resonance condition $\omega_k(|c_k|^2) = \omega_p/2$ could be satisfied for $\omega_p < 2\omega_0$. The SW mode excited in such a case has an evanescent non-propagating character and is localized in the region close to the excitation gate, since it lies below the spectrum of linear propagating SWs.

The excitation thresholds observed in the simulations are $b_{th} = 58, 78, 90\,\mathrm{mT}$ for $\omega_p/2\pi = 12.2, 12.6, 12.8\,\mathrm{GHz}$, while Eq. (6) gives the threshold values of 55, 98, 114 mT, respectively. The overestimation of the threshold for $\omega_p/2\pi = 12.6, 12.8\,\mathrm{GHz}$ in the analytical theory is related to the small theoretical values of the pumping nonadiabaticity $\alpha = |\mathrm{sinc}[kL_g]|$. In these cases $kL_g \simeq \pi/2$ and the theoretical value of the coefficient α is vanishingly small. In reality, the excited SW modes are not ideal plane waves, and they have a finite spread of wave numbers k. Thus, the effective nonadiabaticity parameter α cannot be zero, which results in a lower excitation threshold, as it has been shown in Ref. 37. For the case $\omega_p/2\pi = 12.2\,\mathrm{GHz}$ theoretical value of α is not small and pumping nonadiabaticity is not underestimated, resulting in better theoretical prediction of the threshold.

Similar to the case of the OOP magnetization, the amplitudes of parametrically excited SWs are determined by two mechanisms: (i) the "phase mechanism" related to the 4-wave interaction between the excited SWs, and (ii) the amplitude dependence of the radiation losses existing due to the negative nonlinear frequency shift [23]. The simulated amplitudes of the excited SWs could be adequately described by the theory presented in Ref. 23 with a single fitting coefficients $C_\Sigma = 1.5, 1.2, 1.1$ for $\omega_p/2\pi = 12.2, 12.6, 12.8\,\mathrm{GHz}$, respectively (this fitting parameter depends on the degree of pumping localization and varies in the interval $1 < C_\Sigma < 2$ [23]). At high SW amplitudes theoretical description becomes less accurate, since additional nonlinear SW interaction processes become important. It should be noted, that for the pumping frequency $\omega_p < 2\omega_0$ analytical theory developed in Ref. 23 is not applicable and should be generalized.

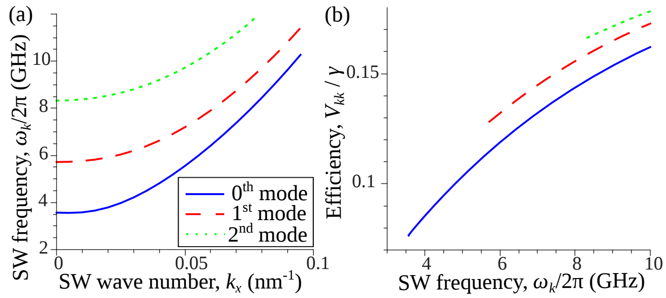

FIG. 4. (a) Spectrum of the 3 lowest SW width modes in a 100 nm wide nanowire waveguide, and (b) efficiency of the parametric excitation of these modes as a function of their frequency. SW spectrum and mode structure in a finite-width waveguide were calculated using Ref. 42 and assuming "free" boundary conditions at the width edges of a nanowire.

IV. NOTES ON MULTIMODE NANOWIRES AND VCMA MATERIALS

All the above presented calculations were made for the *lowest* SW mode, having uniform profile along the nanowire width ($n = 0$). However, with the increase of the nanowire width the higher SW width modes become closer in frequency to the uniform mode, and the parametric resonance condition $\omega_p = 2\omega_{n,k}$ could be satisfied for several SW width modes simultaneously (see an example in Fig. 4(a)). In such a case, it is not clear which SW mode would be excited in the waveguide. To answer this question we plotted the parametric interaction efficiency V_{kk} for different SW width modes in Fig. 4(b). As one can see, at a given frequency V_{kk} has the largest value for the highest SW width mode, since the spatially nonuniform width profile of a higher mode creates a larger dynamic demagnetization field along the y-axis. This results in a larger relative value of the z-component of the dynamic magnetization, and, as was shown above, the interaction efficiency V_{kk} is proportional to this z-component of the dynamic magnetization. Also, at a given frequency higher SW mode has lower k and, thus, lower SW group velocity $v \sim 2\omega_M\lambda_{ex}^2 k$. Thus, the highest mode has the lowest excitation threshold, and will be excited by the parametric pumping. The other SW width modes may be excited only when the highest width mode reaches a sufficiently large amplitude [24]. It should be noted, that the excitation of higher-order modes, having lower group velocity, limits the maximum propagation distance of the excited SWs, which is equal to the propagation length of the highest mode satisfying the conditions of parametric resonance. This property stimulates the use of narrow SW nanowires in which a single-mode propagation regime exists in a wide range of frequencies.

Finally, we note that in all the above presented calculations we used the parameters of a typical VCMA material – Fe-MgO multilayer. These calculations yielded reasonable and experimentally reachable magnitude of the driving microwave electric fields needed for the parametric excitation of propagating SWs using the VCMA effect. Recent experimental and theoretical studies have found (or predicted) materials with substantially better VCMA characteristics, such as $SrTiO_3$/Fe bilayers which has 2 times larger magnetoelectric coefficient β than the Fe/MgO system [43], or Cr/Fe/MgO multilayer having almost 3 times larger β [44]. The use of these novel materials should result in better characteristics of the SW processing devices based on parametric excitation of propagating spin waves through the VCMA effect.

V. SUMMARY

In summary, we have demonstrated that a microwave VCMA pumping could parametrically excite propagating SWs in an ultrathin ferromagnetic nanowire with in-plane static magnetization. The efficiency of the parametric interaction of propagating SWs by the VCMA pumping is proportional to the out-of-plane component of the dynamic magnetization of nanowire. Such type of the parametric coupling is inherent to the case when the pumping is created by the time-dependent anisotropy of the magnetic film, and cannot be realized by application of a microwave magnetic field. The parametric interaction efficiency is nonvanishing in a wide range of the SW wave numbers, including the region of short exchange-dominated SWs, where it tends to be $V_{kk} \to \gamma/4$. This useful property of the VCMA-based parametric excitation of SWs in in-plane magnetized magnetic waveguides provides the practical method of excitation of short SWs, having sufficiently large group velocities for the development of energy-efficient signal processing devices based on exchange-dominated short propagating SWs. The minimum excitation threshold was found to be about 0.5 V/nm in the Fe-MgO nanowire, and this threshold weakly depends on the nanowire width. At a large width of the nanowire, when the nanowire becomes essentially a multimode waveguide, the parametric VCMA pumping excites the highest SW width mode satisfying the parametric resonance condition.

ACKNOWLEDGEMENTS

This work was supported in part by the grant from the Center for NanoFerroic Devices (CNFD) and Nanoelectronics Research Initiative (NRI), by the grant EFMA-1641989 from the National Science Foundation of the USA, by the grant from DARPA, and by the contract from the US Army TARDEC, RDECOM. RV acknowledges support from Ministry of Education and Science of Ukraine, project 0115U002716. The work of M.C. and G.F. was supported by the "Progetto Premiale - SIES Strategic Initiatives for the Environment and Security" and the executive program of scientific and technological cooperation between Italy and China (no. CN16GR09) funded by Ministero degli Affari Esteri e della Cooperazione Internazionale.

* corresponding author, e-mail: verrv@ukr.net

[1] M. Weisheit, S. Fähler, A. Marty, Y. Souche, C. Poinsignon, D. Givord, Electric field-induced modification of magnetism in thin-film ferromagnets, Science **315**, 349 (2007). doi:10.1126/science.1136629.

[2] C.-G. Duan, J. P. Velev, R. F. Sabirianov, Z. Zhu, J. Chu, S. S. Jaswal, E. Y. Tsymbal, Surface magnetoelectric effect in ferromagnetic metal films, Phys. Rev. Lett. **101**, 137201 (2008). doi:10.1103/PhysRevLett.101.137201.

[3] M. Endo, S. Kanai, S. Ikeda, F. Matsukura, H. Ohno, Electric-field effects on thickness dependent magnetic anisotropy of sputtered $MgO/Co_{40}Fe_{40}B_{20}/Ta$ structures, Appl. Phys. Lett. **96**, 212503 (2010). doi:10.1063/1.3429592.

[4] M. Fiebig, Revival of the magnetoelectric effect, J. Phys. D: Appl. Phys. **38**, R123 (2005). doi:10.1088/0022-3727/38/8/R01.

[5] W.-Y. Tong, Y.-W. Fang, J. Cai, S.-J. Gong, C.-G. Duan, Theoretical studies of all-electric spintronics utilizing multiferroic and magnetoelectric materials, Comput. Mater. Sci. **112 (part B)**, 467 (2015). doi:10.1016/j.commatsci.2015.07.016.

[6] F. Matsukura, Y. Tokura, H. Ohno, Control of magnetism by electric fields, Nat. Nanotech. **10**, 209 (2015). doi:10.1038/nnano.2015.22.

[7] S.-S. Ha, N.-H. Kim, S. Lee, C.-Y. You, Y. Shiota, T. Maruyama, T. Nozaki, Y. Suzuki, Voltage induced magnetic anisotropy change in ultrathin $Fe_{80}Co_{20}/MgO$ junctions with Brillouin light scattering, Appl. Phys. Lett. **96**, 142512 (2010). doi:10.1063/1.3385732.

[8] Y. Shiota, S. Murakami, F. Bonell, T. Nozaki, T. Shinjo, Y. Suzuki, Quantitative evaluation of voltage-induced magnetic anisotropy change by magnetoresistance measurement, Appl. Phys. Express **4**, 043005 (2011). doi:10.1143/APEX.4.043005.

[9] T. Nozaki, Y. Shiota, S. Miwa, S. Murakami, F. Bonell, S. Ishibashi, H. Kubota, K. Yakushiji, T. Saruya, A. Fukushima, S. Yuasa, T. Shinjo, Y. Suzuki, Electric-field-induced ferromagnetic resonance excitation in an ultrathin ferromagnetic metal layer, Nat. Phys. **8**, 491 (2012). doi:10.1038/nphys2298.

[10] J. Zhu, J. A. Katine, G. E. Rowlands, Y.-J. Chen, Z. Duan, J. G. Alzate, P. Upadhyaya, J. Langer, P. K. Amiri, K. L. Wang, I. N. Krivorotov, Voltage-induced ferromagnetic resonance in magnetic tunnel junctions, Phys. Rev. Lett. **108**, 197203 (2012). doi:10.1103/PhysRevLett.108.197203.

[11] A. Khitun, M. Bao, K. L. Wang, Magnonic logic circuits, J. Phys. D: Appl. Phys. **43**, 264005 (2010). doi:10.1088/0022-3727/43/26/264005.

[12] A. V. Chumak, V. I. Vasyuchka, A. A. Serga, B. Hillebrands, Magnon spintronics, Nat. Phys. **11**, 453 (2015). doi:10.1038/nphys3347.

[13] Y. Shiota, T. Nozaki, F. Bonell, S. Murakami, T. Shinjo, Y. Suzuki, Induction of coherent magnetization switching in a few atomic layers of FeCo using voltage pulses, Nat. Mater. **11**, 39 (2012). doi:10.1038/nmat3172.

[14] W.-G. Wang, M. Li, S. Hageman, C. L. Chien, Electric-field-assisted switching in magnetic tunnel junctions, Nat. Mater. **11**, 64 (2012). doi:10.1038/nmat3171.

[15] A. Schellekens, A. van den Brink, J. Franken, H. Swagten, B. Koopmans, Electric-field control of domain wall motion in perpendicularly magnetized materials, Nat. Commun. **3**, 847 (2012). doi:10.1038/ncomms1848.

[16] U. Bauer, S. Emori, G. S. D. Beach, Voltage-gated modulation of domain wall creep dynamics in an ultrathin metallic ferromagnet, Appl. Phys. Lett. **101**, 172403 (2012). doi:10.1063/1.4764071.

[17] X. Zhang, Y. Zhou, M. Ezawa, G. P. Zhao, W. Zhao, Magnetic skyrmion transistor: skyrmion motion in a voltage-gated nanotrack, Sci. Rep. **5**, 11369 (2015). doi:10.1038/srep11369.

[18] G. Finocchio, M. Ricci, R. Tomasello, A. Giordano, M. Lanuzza, V. Puliafito, P. Burrascano, B. Azzerboni, M. Carpentieri, Skyrmion based microwave detectors and harvesting, Appl. Phys. Lett. **107**, 262401 (2015). doi:10.1063/1.4938539.

[19] F. H. Tung, G. W. Liang, L. W. Siang, Gateable skyrmion transport via field-induced potential barrier modulation, Sci. Rep. **6**, 21099 (2016). doi:10.1038/srep21099.

[20] K. Nawaoka, Y. Shiota, S. Miwa, H. Tomita, E. Tamura, N. Mizuochi, T. Shinjo, Y. Suzuki, Voltage modulation of propagating spin waves in Fe, J. Appl. Phys. **117**, 17A905 (2015). doi:10.1063/1.4914060.

[21] Y.-J. Chen, H. K. Lee, R. Verba, J. A. Katine, I. Barsukov, V. Tiberkevich, J. Q. Xiao, A. N. Slavin, I. N. Krivorotov, Parametric resonance of magnetization excited by electric field, Nano Lett. **17**, 572 (2017). doi:10.1021/acs.nanolett.6b04725.

[22] R. Verba, V. Tiberkevich, I. Krivorotov, A. Slavin, Parametric excitation of spin waves by voltage-controlled magnetic anisotropy, Phys. Rev. Applied **1**, 044006 (2014). doi:10.1103/PhysRevApplied.1.044006.

[23] R. Verba, M. Carpentieri, G. Finocchio, V. Tiberkevich, A. Slavin, Excitation of propagating spin waves in ferromagnetic nanowires by microwave voltage-controlled magnetic anisotropy, Sci. Rep. **6**, 25018 (2016). doi:

10.1038/srep25018.

[24] V. S. L'vov, Wave Turbulence Under Parametric Excitation (Springer-Verlag, New York, 1994).

[25] T. Brächer, P. Pirro, F. Heussner, A. A. Serga, B. Hillebrands, Localized parallel parametric generation of spin waves in a $Ni_{81}Fe_{19}$ waveguide by spatial variation of the pumping field, Appl. Phys. Lett. **104**, 092418 (2014). doi:10.1063/1.4867982.

[26] A. Capua, C. Rettner, S. P. Parkin, Parametric harmonic generation as a probe of unconstrained spin magnetization precession in the shallow barrier limit, Phys. Rev. Lett. **116**, 047204 (2016). doi:10.1103/PhysRevLett.116.047204.

[27] B. Heinrich, J. F. Cochran, Ultrathin metallic magnetic films: magnetic anisotropies and exchange interactions, Adv. in Phys. **42**, 523 (1993). doi:10.1080/00018739300101524.

[28] H. X. Yang, M. Chshiev, B. Dieny, J. H. Lee, A. Manchon, K. H. Shin, First-principles investigation of the very large perpendicular magnetic anisotropy at Fe|MgO and Co|MgO interfaces, Phys. Rev. B **84**, 054401 (2011). doi:10.1103/PhysRevB.84.054401.

[29] R. Urban, G. Woltersdorf, B. Heinrich, Gilbert damping in single and multilayer ultrathin films: role of interfaces in nonlocal spin dynamics, Phys. Rev. Lett. **87**, 217204 (2001). doi:10.1103/PhysRevLett.87.217204.

[30] L. Udvardi, L. Szunyogh, Chiral asymmetry of the spin-wave spectra in ultrathin magnetic films, Phys. Rev. Lett. **102**, 207204 (2009). doi:10.1103/PhysRevLett.102.207204.

[31] K.-S. Ryu, L. Thomas, S.-H. Yang, S. Parkin, Chiral spin torque at magnetic domain walls, Nature Nanotech. **8**, 527 (2013). doi:10.1038/nnano.2013.102.

[32] R. L. Melcher, Linear contribution to spatial dispersion in the spin-wave spectrum of ferromagnets, Phys. Rev. Lett. **30**, 125 (1973). doi:10.1103/PhysRevLett.30.125.

[33] V. L. Zhang, K. Di, H. S. Lim, S. C. Ng, M. H. Kuok, J. Yu, J. Yoon, X. Qiu, H. Yang, In-plane angular dependence of the spin-wave nonreciprocity of an ultrathin film with Dzyaloshinskii-Moriya interaction, Appl. Phys. Lett. **107**, 022402 (2015). doi:10.1063/1.4926862.

[34] J.-H. Moon, S.-M. Seo, K.-J. Lee, K.-W. Kim, J. Ryu, H.-W. Lee, R. D. McMichael, M. D. Stiles, Spin-wave propagation in the presence of interfacial Dzyaloshinskii-Moriya interaction, Phys. Rev. B **88**, 184404 (2013). doi:10.1103/PhysRevB.88.184404.

[35] R. Verba, V. Tiberkevich, A. Slavin, Influence of interfacial Dzyaloshinskii-Moriya interaction on the parametric amplification of spin waves, Appl. Phys. Lett. **107**, 112402 (2015). doi:10.1063/1.4931089.

[36] M. K. Niranjan, C.-G. Duan, S. S. Jaswal, E. Y. Tsymbal, Electric field effect on magnetization at the Fe/MgO(001) interface, Appl. Phys. Lett. **96**, 222504 (2010). doi:10.1063/1.3443658.

[37] G. A. Melkov, A. A. Serga, V. S. Tiberkevich, Y. V. Kobljanskij, A. N. Slavin, Nonadiabatic interaction of a propagating wave packet with localized parametric pumping, Phys. Rev. E **63**, 066607 (2001). doi:10.1103/PhysRevE.63.066607.

[38] R. V. Verba, Spin waves in arrays of magnetic nanodots with magnetodipolar coupling, Ukrainian J. Phys. **58**, 758 (2013). doi:10.15407/ujpe58.08.0758.

[39] L. Lopez-Diaz, D. Aurelio, L. Torres, E. Martinez, M. A. Hernandez-Lopez, J. Gomez, O. Alejos, M. Carpentieri, G. Finocchio, G. Consolo, Micromagnetic simulations using Graphics Processing Units, J. Phys. D: Appl. Phys. **45**, 323001 (2012). doi:10.1088/0022-3727/45/32/323001.

[40] A. Giordano, G. Finocchio, L. Torres, M. Carpentieri, B. Azzerboni, Semi-implicit integration scheme for Landau-Lifshitz-Gilbert-Slonczewski equation, J. Appl. Phys. **111**, 07D112 (2012). doi:10.1063/1.3673428.

[41] P. Krivosik, C. E. Patton, Hamiltonian formulation of nonlinear spin-wave dynamics: Theory and applications, Phys. Rev. B **82**, 184428 (2010). doi:10.1103/PhysRevB.82.184428.

[42] K. Y. Guslienko, A. N. Slavin, Magnetostatic Green's functions for the description of spin waves in finite rectangular magnetic dots and stripes, J. Magn. Magn. Mater. **323**, 2418 (2011). doi:10.1016/j.jmmm.2011.05.020.

[43] I. Kota, H. Imamura, Electric field effect on magnetic anisotropy in Fe-monolayer on $SrTiO_3$ and MgO insulating layer: A first-principles study, in: Magnetism and Magnetic Materials Conference (Honolulu, HI, USA, Nov 3-7 2014), pp. CE–11.

[44] T. Nozaki, A. Kozioł-Rachwał, W. Skowroński, V. Zayets, Y. Shiota, S. Tamaru, H. Kubota, A. Fukushima, S. Yuasa, Y. Suzuki, Large voltage-induced changes in the perpendicular magnetic anisotropy of an MgO-based tunnel junction with an ultrathin Fe layer, Phys. Rev. Applied **5**, 044006 (2016). doi:10.1103/PhysRevApplied.5.044006.